

# V-BAND ON-WAFER NOISE PARAMETER MEASUREMENTS

M. Lahdes, J. Tuovinen

MilliLab, VTT Information technology,  
P.O.Box 1202, FIN-02044 VTT, Finland  
e-mail: manu.lahdes@vtt.fi

## ABSTRACT

*Different noise parameter measurement methods and receiver requirements are discussed. A set-up for on-wafer V-band noise parameter measurements using so called cold-source method is presented. The operation of the system is demonstrated by showing experimental results of a InP HEMT (58-62 GHz) and a passive component (51-66 GHz).*

## INTRODUCTION

Advances in semiconductor technologies has resulted a growing interest towards MMIC-applications at mm-wave frequencies. Designing these applications require a full characterization of electrical properties of the active and passive components. Noise performance of an active device, usually a transistor, is an important factor in successful design. Therefore, obvious needs exists for accurate measurement of the on-wafer noise parameters. Carrying out these measurements at mm-wave frequencies in an on-wafer environment is challenging compared to the microwave frequencies where noise parameter measurement techniques are quite established.

The dependence of the noise figure of a linear two-port on the source admittance is given by

$$F = F_{\min} + R_n \frac{\left\{ (G_s - G_{\text{opt}})^2 + (B_s - B_{\text{opt}})^2 \right\}}{G_s} \quad (1)$$

where

$F_{\min}$  = minimum noise figure of the device

$G_{\text{opt}} + jB_{\text{opt}}$  = source admittance for minimum noise figure

$R_n$  = noise resistance

$G_s + jB_s$  = source admittance.

In a noise parameter measurement different source impedances are presented to the device under test (DUT) and corresponding noise figures are measured. There are four unknown noise parameters  $F_{\min}$ ,  $R_n$ ,  $G_s$ , and  $B_{\text{opt}}$  so a minimum of four measurements are required. However, in order to minimize the effects of the measurement errors, additional measurements are done and curve fitting is applied. Cold-source measurement method [1] is used to measure the noise parameters of the DUT. The technique presented in [2] has been improved. The new technique [3] corrects effects of reflection coefficient difference of the noise source between on and off states. A further improvement takes into account losses of the passive network between the DUT and the receiver [3]. Only a simple 1-port tuner is needed in this method. The current status of the test facility for measuring transistor noise properties on-wafer in V-band is described.



## MEASUREMENT METHODS

Several different methods which can be used to measure the noise parameters of the DUT exists. These can be separated from each other by the tuner type, and the noise figure measurement method used. The tuners can be 1-port, 2-port, electrical, mechanical, automatic, or manually operated. The noise figure can be measured with the traditional Y-method or with a so called cold source method. In this method two different noise temperatures are introduced to the receiver (Y-method) during the receiver calibration, but during the DUT noise measurements only the passive input network acts as a noise source at an ambient temperature [1-3]. In Fig.1, different kind of measurement set-ups are presented. Fig.1a shows so called classical method. It has been widely used for measurements at microwave frequencies [4]. The set-up can be made more practical by adding two waveguide switches, see Fig.1b. This setup can be used for both classical and cold-source method [5]. When cold-source method is used, the tuner input port is switched to a termination and it acts as an 1-port tuner. The noise power can be also injected through a directional coupler as presented in Fig.1c [6], but the use of coupler adds loss to the system, thus limiting the tuning range. The system used in our measurement is presented in Fig.1d [3]. It uses a simple uncalibrated manual tuner, see Fig.2, and the noise figure measurement method is the cold-source method. The use of an uncalibrated tuner is made possible by relocating the switch 1. Now each tuner setting are measured with the VNA and the tuner repeatability depends only on the repeatability of the waveguide switch. The noise source is located at receiver side of the DUT. This means that the receiver can be calibrated any time during long measurement sessions to reduce the effects of drifting. Also, tunerless methods based on measuring noise figure with 50 ohm input load (F50 method) over a wide bandwidth and fitting a noise model has been developed [7-9]. Obvious advantages are simpler setup and disadvantages are the need to know of the transistor noise model and capability of wideband measurements.

## TUNERS

The most important property of a calibrated tuner is the repeatability, in other words, its ability to re-produce the same impedances during the measurements as was recorded in the calibration. In practice, this means that some automated tuner system is needed. Good repeatability can be achieved with manual tuners also, but this can be very time consuming. At V-band only mechanical automated tuners are commercially available. Uncalibrated tuners can be used as presented in this paper.

One of the main complication of noise parameter measurements as frequency increases is the increasing loss between the impedance tuner and DUT. It is essential to minimize this loss and to have the tuner as close as possible to the DUT. Ideally, an active probe tip with an impedance tuner should be used, as developed at the U. of Leeds. However, these are not available in a practical form yet. The loss between the tuner and DUT reduces the maximum magnitude of the reflection coefficient or in other words the range of impedances possible to create in the input of the DUT. In the set-up used here magnitudes of  $|\Gamma_s| \leq 0.7$  are reached.

## RECEIVER

A good receiver should have low noise, high gain, good matching, high linearity, and good stability. These properties are not easily achieved at mm-wave frequencies. Use of a high quality LNA with sufficient gain is highly recommended. The LNA will minimize the noise contribution of the latter stages of the receiver, for example the mixer stage. In the noise measurements single side band (SSB) measurements are preferred. One method to achieve this is to choose the first IF so that the image frequency is below the cut-off frequency of the wave guide [3,6]. In a wideband system



making SSB measurements is difficult. In DSB measurements both side bands should be as identical as possible. This is done by selecting a low IF to put the side bands close together. If an isolator is connected to the input port of the receiver only the noise figure and reflection coefficient measurements are sufficient. Without the isolator a full set of the receiver noise parameters must be measured. The isolator will degrade the noise performance of the receiver but will simplify the measurement procedure.

Fig.2 shows the wideband setup for 50–75 GHz under development. This is a similar system used for W-band measurements at the U. of Leeds [5]. In the wideband setup, the receiver is based on the fundamental mixer with an IF of 10 MHz. The LO is a commercial product and is programmable. The bias of the mixer is fixed. The noise figure of the mixer is expected to be about 10 dB. Because of this, the LNA in front of the mixer is very desirable. A wideband LNA based on InP MMICs is foreseen through the on going Planck LFI 70 GHz receiver development work in-house [10]. Currently a substitute LNA [11] is used which allows operation between 51–66 GHz.

## MEASUREMENT PROCEDURE

Before the actual noise measurements are carried out, the test system must be fully characterized. Characterization includes measurements of passive networks between reference planes A-B, C-E, D-E, and the reflection coefficients of the receiver and noise-source (both hot and cold states) and calibration of the receiver. This is described in detail in [3]. The receiver calibration includes the measurement of the gain-bandwidth constant kBG by connecting the noise source to the receiver via switch 2 and then the calculation of the receiver noise figure from the kBG measurements [12].

After the system characterization and the receiver calibration the setup is set for noise measurements. The configuration is presented in Fig.2. The DUT is placed into the probe station and set to the operating point of interest. The VNA is switched to the DUT and the 2-port S-parameters are measured. Noise figure measurements are done in two steps. First, the VNA is connected to the tuner via switch 1, the tuner is set and its reflection coefficient is measured. Then the tuner is switched to the DUT and the noise power is measured as a function of the frequency. The procedure is repeated for all the selected source impedance points. The noise figure of the entire system is given by

$$F_{tot,i} = \frac{P_i |1 - S_{11} \Gamma_i|^2 |1 - \Gamma_s \Gamma_{rcv}|^2 |1 - S_{11OUT} \Gamma_2|^2}{T_0 kBG |S_{21}|^2 (1 - |\Gamma_i|^2) |S_{21OUT}|^2} - \frac{T_a}{T_0} + 1 \quad i = 1, 2, 3, \dots \quad (2)$$

where  $P_i$  is the measured noise power,  $\Gamma_i$  is the source reflection coefficient of the DUT,  $S_{ij}$  are the S-parameters of the DUT,  $S_{ijOUT}$  are the S-parameters of the output network C-E and  $\Gamma_2$  is the output reflection coefficient of the DUT. The actual source reflection coefficient  $\Gamma_i$  seen by the DUT calculated from the measured reflection coefficient at the tuner reference plane A and the S-parameter data of A-B network acquired during the system characterization. The noise figure of the DUT is calculated using the Friis formula [13] as follows,

$$F_{DUT} = F_{tot} - \frac{F_{rcv} - G_{aOUT}}{G_{aDUT} G_{aOUT}}, \quad (3)$$

where  $F_{rcv}$  in the noise figure of the receiver,  $G_{aDUT}$  is the available gain of the DUT,  $G_{aOUT}$  is the available gain of the output network C-E. As a result we get the noise behavior of the DUT as a function of source impedance. The noise parameters are extracted using the least-squares fitting method [14] for all the measurement frequencies.



## MEASUREMENT RESULTS

As an example of the measurement capabilities, the results of an InP HEMT (58-62 GHz) are shown in Figures 3 and 4. The minimum noise figure varies between 2.0 and 2.7 dB. The mean value is 2.35 dB. The estimated uncertainty of the result is  $\pm 0.5$  dB ( $2\sigma$ ). The uncertainty estimation is done by Monte Carlo analysis [15]. Density histograms of this analysis (at 60 GHz) of the magnitude and the angle of the optimum reflection coefficient are presented in Fig. 5 and 6 respectively. Also a 10 dB attenuator was measured with the set-up under development (51-66 GHz). The measured noise parameters are presented in Fig. 7-10. For comparison parameters calculated from the S-parameters are also plotted.

## CONCLUSIONS

A system for on-wafer V-band noise parameter has been presented. The operation of the set-up and measurement method has been demonstrated by experimental data of both active and passive components.

## REFERENCES

- [1] Adamian V.,Uhlir A.: "A novel procedure for receiver noise characterization", *IEEE Transactions on Instrumentation and measurement*, vol. 22, no. 2, pp.181-183, 1973.
- [2] Meierer R., Tsironis C.: "An on-wafer noise parameter measurement technique with automatic receiver calibration", *Microwave Journal*, vol. 38, no. 3, pp.22-37, 1995.
- [3] Lahdes M., Tuovinen J., Sipilä M.: "60 GHz on-wafer noise parameter measurements using cold-source method", 49th ARFTG Conference Digest, pp. 146-154, 1997.
- [4] Sannino M.: "On the determination of device noise and gain parameters", *Proceedings of the IEEE*, vol. 67, no. 9, s.1364-1366, 1979.
- [5] Alam T.A., Pollard R.D., Snowden C.M.: "Determination of W-band noise parameters", *Electronic Letters*, vol. 34, no. 3, pp.288-289, 1998.
- [6] Webster R. T., Slobdnik A. J., Roberts G. A.: "Determination of InP HEMT noise parameters and S-parameters to 60 GHz", *IEEE Transactions on Microwave Theory and Techniques*, vol.43, no.6, pp.1216-1225,1995.
- [7] Pospiezalski M.: "Modelling of noise parameters of MESFETS's and MODFET's and their frequency and temperature dependence", *IEEE Transactions on Microwave Theory and Techniques*, vol. 37, no. 9, pp.1340-1350, 1989.
- [8] Tasker P. J., Reinert W., Hughes B., Braunstein J., Schechtweg M.: "Direct extraction of all four transistor noise parameters using a 50 ohm measurement system", *IEEE MTT-S International Microwave symposium*, 1993.

- [9] Lazaro A., Pradell L., Beltran A., O'Callaghan J. M.: "Direct extraction of all four transistor noise parameters from 50 ohm noise figure measurements", *Electronic Letters*, vol. 34, no. 3, pp.289-291, 1998.
- [10] "Planck Low Frequency Instrument proposal submitted to European Space agency for the FIRST/Planck programme". Part I: Scientific and Technical Plan. Feb. 1998.
- [11] Lunden O.P., Sipilä M., Jenu M.: "60 GHz LNAs using commercially available PM HEMTs", *Microwave Journal*, vol. 38, no. 3, pp.80-88, 1995.
- [12] Strid E.: "Noise measurements for low-noise GaAs FET amplifiers", *Microwave System News*, vol. 10, s. 62-70, 1981.
- [13] Friis H. T. : "Noise figures of radio receivers", *Proceedings of the IRE*, vol. 32, no. 7, s. 419-422, 1944.
- [14] Lane R. Q.: "The determination of device noise parameters", *Proceedings of the IEEE*, vol. 57, no. 8, pp. 1461-1462, 1969.
- [15] Lahdes M.: "Uncertainty analysis of V-band On-wafer Noise Parameter Measurement System", to be published in the *Proceedings of the 28th European Microwave Conference*, Amsterdam, 1998.

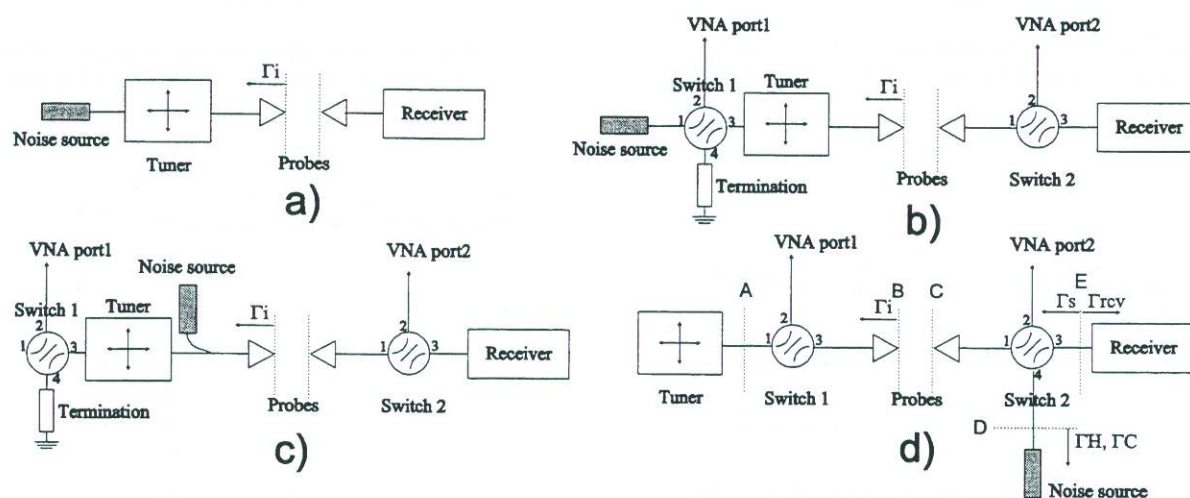


Fig.1: Different noise parameter measurement methods. The method used in this paper is shown in d).

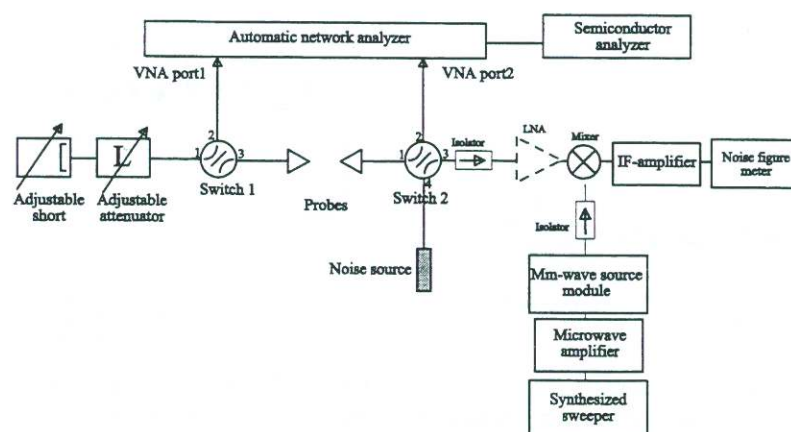


Fig.2: Noise parameter measurement set-up under development.



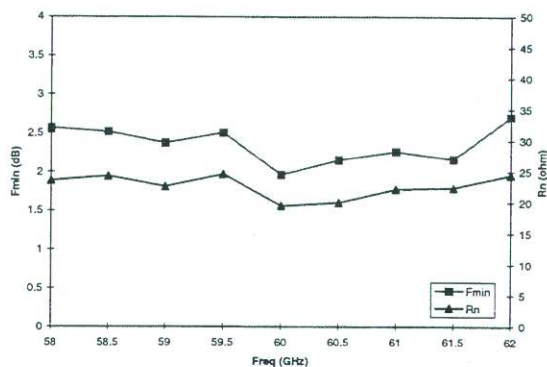


Fig.3: The measured minimum noise figure  $F_{\min}$  and noise resistance  $R_n$ .

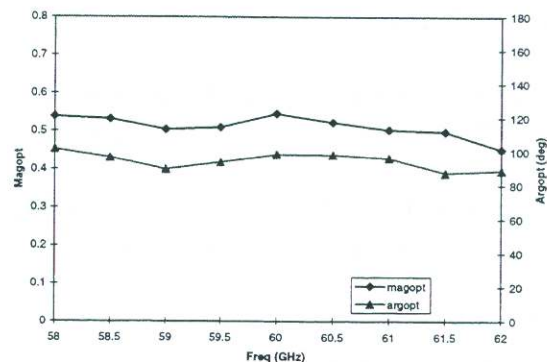


Fig.4: The measured magnitude and phase of the optimum source reflection coefficient.

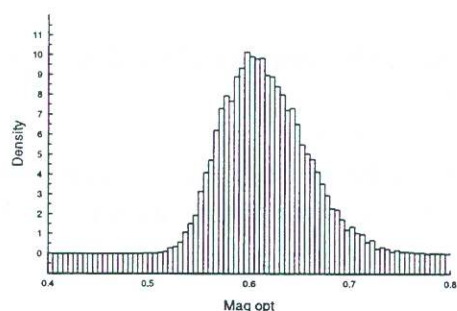


Fig.5: Monte-Carlo analysis results. Scattering of the optimum magnitude of the source reflection coefficient.

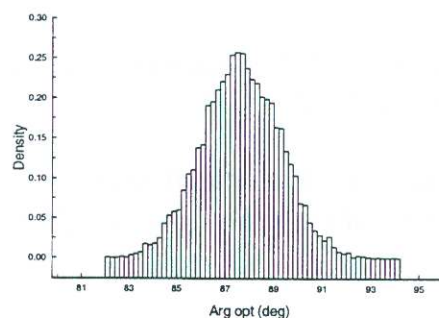


Fig.6: Monte-Carlo analysis results. Scattering of the optimum angle of the source reflection coefficient.

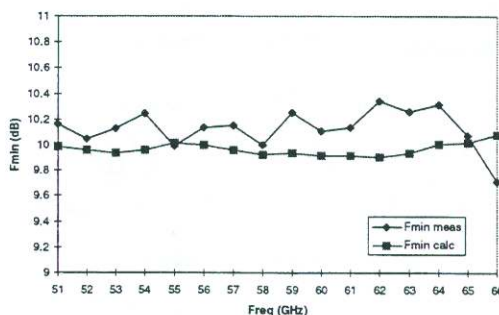


Fig.7: The measured and calculated (from S-param.) minimum noise figure  $F_{\min}$  of a 10 dB attenuator.

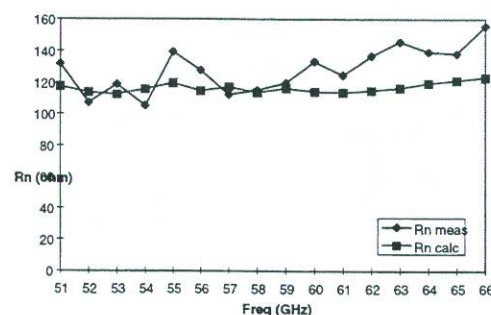


Fig.8: The measured and calculated (from S-param.) noise resistance  $R_n$  of a 10 dB attenuator.

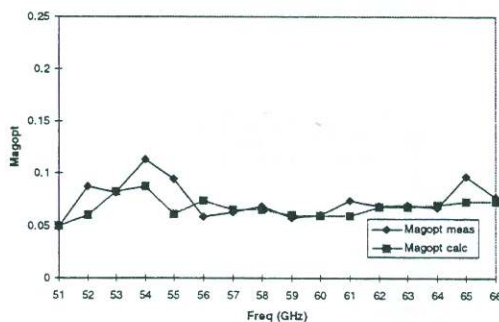


Fig.9: The measured and calculated (from S-param.) magnitude of the optimum source reflection coefficient.

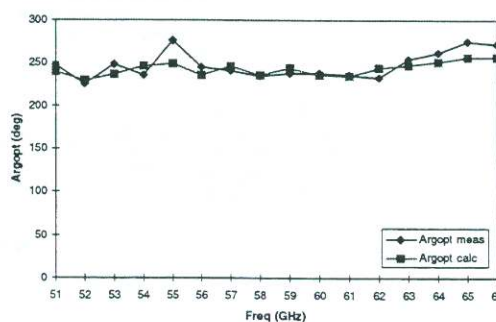


Fig.10: The measured and calculated (from S-param.) angle of the optimum source reflection coefficient.